ACI STRUCTURAL JOURNAL TECHNICAL PAPER

Title no. 104-S46

Tensile-Headed Anchors with Large Diameter and Deep Embedment in Concrete

by Nam Ho Lee, Kang Sik Kim, Chang Joon Bang, and Kwang Ryeon Park

This paper presents test results for large cast-in-place anchor bolts in concrete. The tests were performed to evaluate the tensile performance of large anchors, that is, anchors with a diameter greater than 2 in. (50 mm) or an embedment depth greater than 25 in. (635 mm), which are not addressed by ACI 318, Appendix D, and ACI 349, Appendix B. The tests were also intended to investigate the safety of such anchors for use in nuclear power plants and the effects of regular (conventional) and special reinforcement on the strength of such anchors. The test results are used to assess the applicability of existing design formulas valid for smaller anchors to large anchors. Suggestions are made for incorporating the effects of deep embedment or large diameter in existing design provisions for cast-in-place tensile anchor bolts under tension load.

Keywords: anchor; anchor bolt; cast-in-place; embedment; tension test.

INTRODUCTION

Current anchorage designs for nuclear power plants in Korea use large anchor bolts with diameters exceeding 2 in. (50 mm), embedment depths exceeding 25 in. (635 mm), a specified yield strength of 140 ksi (980 MPa), and a specified ultimate strength of 155 ksi (1085 MPa). Whereas the tensile behavior of smaller anchors has been studied extensively, large anchors have not been adequately addressed. In the research described herein, large anchors were tested in tension to develop design criteria for anchors that are not addressed by ACI 318-05, Appendix D,[1] or ACI 349-01, Appendix B,[2] and to evaluate the applicability of capacity-prediction methods developed for smaller anchors.

To evaluate the tensile behavior of anchors with large diameters and embedment depths, various anchors, with diameters from 2.75 to 4.25 in. (69.9 to 108 mm) and embedment depths from 25 to 45 in. (635 to 1143 mm) were tested.

RESEARCH SIGNIFICANCE

The research described herein is the first experimental information on the tensile behavior of very large headed anchor bolts ($h_{ef} \geq 21$ in. [525 mm]). It is important because although such anchor bolts are commonly used in power plants and for the anchorage of tanks, no design provisions validated by tests exist for them.

EXISTING FORMULAS FOR PREDICTING TENSILE CAPACITY OF ANCHOR BOLTS IN CONCRETE

Presuming the head of the anchor is large enough to prevent pull-out failure (refer to ACI 318, Appendix D), the tensile capacity of large anchor bolts is governed by tensile yield and fracture of the anchor steel or by tensile breakout of the concrete in which the anchor is embedded. Steel yield and fracture are well understood. The breakout formulas of current U.S. design provisions (ACI 318-05[1] and ACI 349-01[2]) are based on the concrete capacity design (CCD) method (CCD method),[3] which is a derivative of the Kappa method[4] described in Reference 5.

According to the CCD method, the average concrete breakout capacity of headed anchors in uncracked concrete is given by Eq. (1). This equation is valid for anchors with a relatively small head (mean bearing pressure at breakout load of approximately $13f_c'$).[3] In ACI 318, Appendix D,[1] the 5%-fractile of the concrete cone breakout loads are predicted, which is assumed as 0.75 times the mean value. This leads to Eq. (2). ACI 318-05, Appendix D,[1] allows the use of Eq. (4) for calculating the nominal breakout capacity of headed anchors with an embedment depth $h_{ef} \geq 11$ in. (279 mm) in uncracked concrete. Equation (4) modifies the CCD method slightly by changing the exponent on the embedment depth h_{ef} from 1.5 to 1.67. The mean concrete capacity may be calculated according to Eq. (3). In ACI 349-97,[6] a 45-degree cone model is used to calculate the concrete breakout capacity (Eq. (5)). Because Eq. (5) was used in design, it may be considered to predict approximately the 5%-fractile of test results. A summary of the proposed predictors are given as

Equation number	Predictor	Remark
(1)	$N_{u,m} = 40\sqrt{f_c'}\,h_{ef}^{1.5}$ (lb)	Mean breakout strength, CCD-method with exponent 1.5 on h_{ef}
(2)	$N_u = 30\sqrt{f_c'}\,h_{ef}^{1.5}$ (lb)	Nominal breakout strength, ACI 318-05, Appendix D
(3)	$N_{u,m} = 26.7\sqrt{f_c'}\,h_{ef}^{1.67}$ (lb)	Mean breakout strength for anchors with $h_{ef} \geq 10$ in. (254 mm), CCD-method with exponent 1.67 on h_{ef}
(4)	$N_u = 20\sqrt{f_c'}\,h_{ef}^{1.67}$ (lb)	Nominal breakout strength for anchors with $h_{ef} \geq 10$ in. (254 mm) according to ACI 318-05, Appendix D
(5)	$N_u = 4\sqrt{f_c'}\pi h_{ef}^2\,(1 + d_k/h_{ef})$ (lb)	Nominal breakout strength, ACI 349-97 (45-degree cone model)

Note: f_c' = specified concrete compressive strength (psi); h_{ef} = effective embedment (in.); and d_b = diameter of anchor head (in.).

DESCRIPTION OF EXPERIMENTAL PROGRAM

Test specimens

To evaluate the effects of embedment depth, anchor diameter, and supplementary reinforcement patterns on the tensile capacity of large anchors, five different test configurations were selected and four test replicates with each configuration

ACI Structural Journal, V. 104, No. 4, July-August 2007.
MS No. S-2006-232 received June 6, 2006, and reviewed under Institute publication policies. Pertinent discussion including author's closure, if any, will be published in the May-June 2008 *ACI Structural Journal* if the discussion is received by January 1, 2008.

ACI member **Nam Ho Lee** *is a Senior Research Engineer in the Civil Engineering Department of the Korea Power Engineering Co. He received his BS from Seoul National University and his MS and PhD from the Korea Advanced Institute of Science & Technology. He is a member of ACI Committees 349, Concrete Nuclear Structures, and 355, Anchorage to Concrete, and Joint ACI-ASME Committee 359, Concrete Components for Nuclear Reactors. His research interests include the nonlinear behavior of concrete structures and anchorage to concrete.*

Kang Sik Kim *is a Senior Researcher, Environment and Structure Laboratory, Korea Electric Power Research Institute, Daejeon, Korea. His research interests include the behavior of concrete-filled steel plate structures and anchorage to concrete.*

Chang Joon Bang *is a Project Engineer at Korea Hydro & Nuclear Power Co. Ltd., Seoul, Korea. He is currently a Graduate Student of civil engineering, Lehigh University, Bethlehem, Pa.*

Kwang Ryeon Park *is a Research Engineer, Civil Engineering Department, Korea Power Engineering Co.*

were performed giving 20 specimens in total. The test program is summarized in Table 1. The test specimens are shown in Fig. 1. All anchors were fabricated of ASTM A540 Gr. B23 Class 2 steel (equivalent to ASME SA 549 Gr. B23 Class 2 used in Korean nuclear power plants) with f_y = 140 ksi (980 MPa) and f_u = 155 ksi (1085 MPa). The anchor head consisted of a round thick plate which was fixed to the bolt by clamping nuts (Fig. 2). The diameter of the round plate was d_h = 6 in. (152.4 mm) (d_b = 2.75 in. [69.9 mm]), d_h = 8.5 in. (215.9 mm) (d_b = 3.75 in. [95.3 mm]), and d_h = 10 in. (254.0 mm) (d_b = 4.25 in. [108.0 mm]). The size of the concrete test block was large enough to avoid splitting failure. The concrete volume (width/length/depth) available for each anchor is shown in Table 1. Furthermore, to minimize the width of eventual shrinkage cracks, the top and bottom of the test member were reinforced in both directions with No. 10 bars at 16, 10, and 10 in. (406.4, 254, and 254 mm) spacing for Specimens T1, T2, and T3, respectively. This surface reinforcement does not significantly influence the concrete breakout load. As shown in Fig. 1, wooden and steel frames were constructed to suspend the cast-in-place anchors in the correct position and at the correct embedment depth. The concrete mixture for the test specimens is shown in Table 2(a). The concrete used in the test specimens was comparable to the concrete used in the Korean Nuclear Plant, except that 20% by weight of the Type I cement was substituted by fly ash and 1 in. (25 mm.) crushed aggregate was used instead of 3/4 in. (19 mm). The target concrete strength at 42 days was f'_c = 5500 psi (37.9 MPa). The actual concrete strength at the time of testing is given in Table 2(b). The concrete for the specimens of one test series was placed from one batch. Whereas in test Series T1 to T3, no special reinforcement was used to resist the applied tension load, in test Series T4 and T5, supplementary reinforcement (refer to Fig. 3) was used to increase the ultimate load. The supplementary reinforcements consisted of vertical stirrups (eight No. 8 bars and 16 No. 8 bars for test Series T4 and T5, respectively), as shown in Fig. 3.

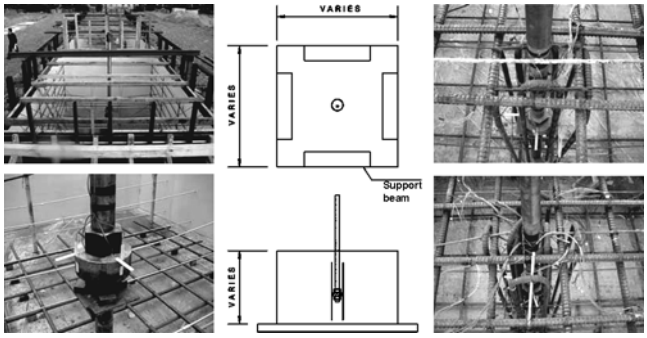

Fig. 1—Tension test Specimens T1, T2, T3, T4, and T5.

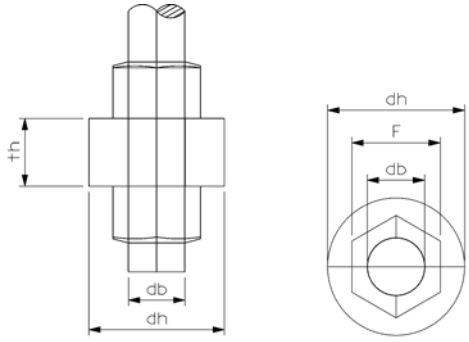

Anchor Diameter db, in. (mm)	Plate Diameter dh, in. (mm)	Plate thickness th, in. (mm)	Nut width F, in. (mm)
2.75 (69.9)	6.0 (152.4)	3.0 (76.2)	3.875 (98.4)
3.75 (95.3)	8.5 (215.9)	4.0 (10.6)	5.375 (136.5)
4.25 (108.0)	10.0 (254.0)	5.0 (127.0)	6.875 (17.6)

Fig. 2—Details of anchor head.

Table 1—Description of tension test specimens

Specimen	Reinforcement	Anchor diameter, d_b, in. (mm)	Diameter of anchor head, d_h, in. (mm)	Effective embedment h_{ef}, in. (mm)	Concrete volume available for each anchor (width/length/depth)
T1-A,B,C,D	None	2.75 (69.9)	6.0 (152.4)	25 (635)	$5.9h_{ef}$ /$5.0h_{ef}$/ $2.9h_{ef}$
T2-A,B,C,D	None	3.75 (95.3)	8.5 (215.9)	35 (889)	$5.4h_{ef}$/$4.7h_{ef}$/ $2.0h_{ef}$
T3-A,B,C,D	None	4.25 (108.0)	10.0 (254.0)	45 (1143)	$5.0h_{ef}$/$3.6h_{ef}$/ $2.0h_{ef}$
T4-A,B,C,D	Supp. No. 1	2.75 (69.9)	6.0 (152.4)	25 (635)	$5.9h_{ef}$/$5.0h_{ef}$/ $2.9h_{ef}$
T5-A,B,C,D	Supp. No. 2	2.75 (69.9)	6.0 (152.4)	25 (635)	$5.9h_{ef}$/$5.0h_{ef}$/ $2.9h_{ef}$

Table 2(a)—Concrete mixture proportioning

Nominal strength, psi, at 42 days	W/ (C + FA)	S/a, %	W, lb	C, lb	FA, lb	S, lb	G, lb	WRA,* mL	AEA,† mL
5500	0.44	44	525	514	128	1257	1617	474	26

*Water-reducing admixture.
†Air-entraining admixture.

Table 2(b)—Concrete strength at time of testing

Test specimen	Curing ages, days	Compressive strength, psi (MPa)
T1-A/B/C/D	58/50/44/42	5771 (39.8)/5630 (38.8)/ 5508 (38.0)/5464 (37.7)
T2-A/B/C/D	41/45/47/49	5177 (35.7)/5248 (36.2) / 5291 (36.5)/5320 (36.7)
T3-A/B/C/D	61/56/54/50	5448 (37.6)/5348 (36.9) / 5305 (36.6)/5220 (36.0)
T4-A/B/C/D	57/55/54/50	5945 (41.0)/5917 (40.8)/ 5903 (40.7)/5817 (40.1)
T5-A/B/C/D	71/70/69/68	6144 (42.4)/6130 (42.3)/ 6130 (42.3)/6116 (42.2)

Test setup

The test setup consisted of a loading frame, loading plate, jack assembly, load cell, and other items, as shown in the schematic and photo in Fig. 4. The load was applied to the anchor under force-control in an increment of approximately 3.5% of ultimate steel strength of the anchor bolt (F_u = 925, 1683, and 2192 kips [4114.6, 7486.4, and 9750.5 kN], for bolts with a diameter of 2.75, 3.25, and 4.25 in. [69.90, 82.55, and 107.95 mm], respectively), that is, 30, 60, 77, 68, and 48 kips (133.4, 266.9, 342.5, 302.5, and 213.5 kN) for Series T1, T2, T3, T4, and T5, respectively. It was reacted in two directions by a stiff frame to minimize the bending moment in the test specimen. The clear distance between the supports was 4.0 h_{ef} for Specimens T1 through T5, thus allowing for an unrestricted formation of a concrete cone. The applied load was measured by a load cell. Additionally, the strain along the embedment length of the anchor bolt was measured (Fig. 5). Furthermore, the displacement of the top end of the anchor was measured by LVDTs (Fig. 5).

TEST RESULTS

Failure loads, failure modes and load displacement behavior

The average failure loads are summarized in Table 3(a) (Series T1 to T3) and Table 3(b) (Series T4 and T5). The values given in the tables are normalized to f_c' = 5500 psi (37.9 MPa) by multiplying the measured peak load of each test with the factor $(5500/f_{c,test})^{0.5}$. In test Series T1 to T3, failure was caused by concrete cone breakout well below the anchor bolt steel capacities (F_u = 925, 1683, and 2192 kips [4114.6, 7486.4, and 9750.5 kN] for bolts with diameters of 2.75, 3.25, and 4.25 in. [69.90, 82.55, and 107.95 mm], respectively). The cracking patterns in the specimen after the test are depicted in Fig. 6(a). Generally, one major longitudinal crack was observed, centered approximately on the sides of the block, in combination with a horizontal crack and some transverse cracks. On the top surface of the block, the cracks formed a circular pattern around the anchor. To identify the internal crack propagation defining the roughly conical breakout body, one replicate of each specimen type was selected, and the concrete was cored on two orthogonal planes whose intersection coincided with the axis of the anchor. The cores confirmed a breakout cone whose angle with the concrete surface varied from α = 20 to 30 degrees, following the typical crack profiles shown in Fig. 6(b).

In general, test Specimens T4 and T5, with supplementary reinforcement (Fig. 3), were not tested to failure. At the applied peak load, the measured steel strains exceeded the yield strain and because of safety concerns a sudden rupture of the bolt was avoided. Only Specimen T4-A was tested to

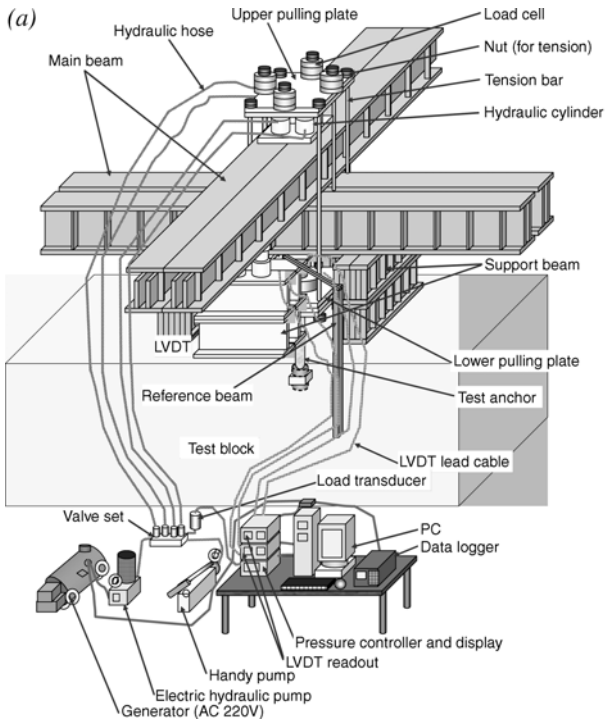

Fig. 4—Tension test setup: (a) schematic; and (b) photo.

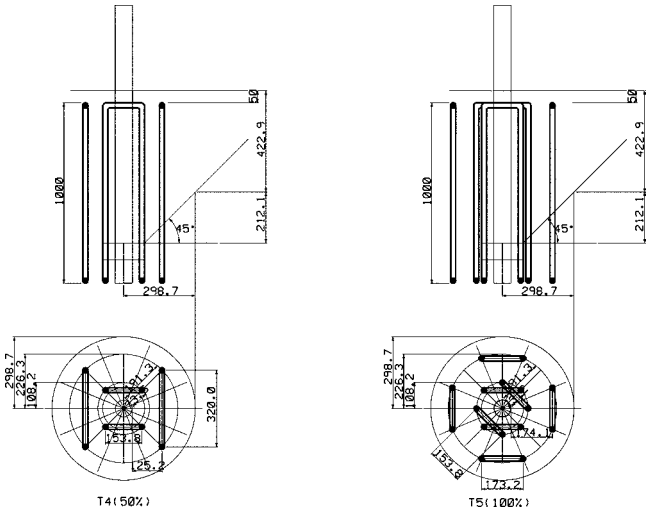

Fig. 3—Supplementary reinforcement in Specimens T4 and T5.

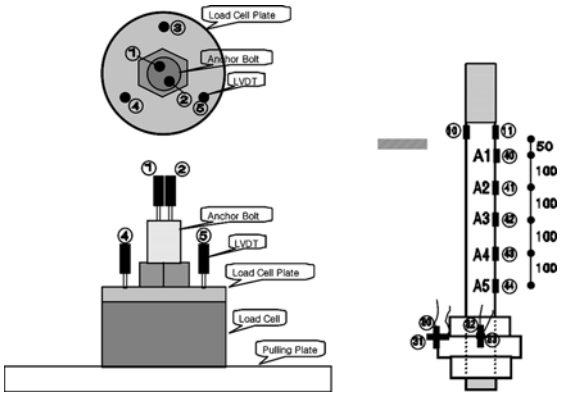

Fig. 5—Location of LVDTs and strain gauges (Specimen T1).

Table 3(a)—Tension test results and predictions for unreinforced Specimens T1, T2, and T3

Classification	Reference	Concrete breakout capacities, kips (kN), by embedment		
		Specimen T1 25 in. (635 mm)	Specimen T2, 35 in. (889 mm)	Specimen T3, 45 in. (1143 mm)
Predictions	ACI 349-97, Eq. (5)	676 (3006)	1305 (5804)	2138 (9510)
	ACI 318-05, Eq. (4)	320 (1423)	562 (2499)	855 (3803)
	CCD method with $h_{ef}^{1.5}$ Eq. (1)	371 (1650)	614 (2731)	895 (3981)
	CCD method with $h_{ef}^{1.67}$ Eq. (3)	428 (1903)	750 (3336)	1142 (5079)
Tests	Mean	509 (2264)	744 (3309)	1242 (5524)
	COV, %	5.8	2.8	6.1
	5%-fractile	393 (1748)	662 (2944)	944 (4199)
	5%-fractile/ mean	0.77	0.89	0.76

Classification	Symbol in Fig. 9	Comparison	Ratios of observed to predicted capacities			
			Specimen T1 25 in. (635 mm)	Specimen T2, 35 in. (889 mm)	Specimen T3, 45 in. (1143 mm)	Mean
5% fractile of test results	(I)	$Nu_{,5\%}$/ Eq. (5)	0.58	0.51	0.44	0.51
	(II)	$Nu_{,5\%}$/ Eq. (4)	1.24	1.19	1.12	1.18
Mean of test results	(III)	Mean/ Eq. (1)	1.37	1.21	1.39	1.32
	(IV)	Mean/ Eq. (3)	1.19	0.99	1.09	1.09

failure. Failure of this specimen was caused by forming a concrete cone. From the load-displacement curves (Fig. 7), it can be concluded that in test Series T4, the applied maximum loads were almost identical with the failure loads. In test Series T5, however, the failure load of the anchors was not reached. Because Specimens T4 and T5 showed no cracking at the concrete surface, no cores were taken to check whether a cone had begun to form.

The load-displacement curves for Specimens T1, T2, T3, T4, and T5 are shown in Fig. 7(a) through 7(e), using the displacement measured at the top of each anchor. The load-displacement relationship for each test replicate varied based on the concrete strength at the time of testing. The projecting lengths of the anchor shafts from the concrete surface to the top of the anchor for Specimens T1, T2, T3, T4, and T5 were 41.7, 48.6, 53.1, 41.7, and 41.7 in. (1059, 1234, 1348, 1059, and 1059 mm), respectively. Because the measured displacements shown in Fig. 7 include the steel elongation of the projecting anchor length, the actual anchor displacements at the top of the concrete surface, which are accumulated along the embedded portion of the anchor, are much smaller than shown in Fig. 7. In Fig. 8, the relationship between load and anchor displacement at the surface of the concrete (calculated from the displacements measured at the anchor top end subtracting the steel elongation of the projecting length) are plotted for test Series T1 to T5. In some tests, the calculated displacements at the concrete surface are negative for low loads. It is believed that this is

Table 3(b)—Tension test results and predictions for reinforced Specimens T4 and T5

Classification	Reference	Concrete breakout capacities, kips (kN), by embedment		
		Specimen T4 25 in. (635 mm)	Specimen T5, 25 in. (635 mm)	Specimen T1, 25 in. (635 mm)
Predictions	ACI 349-97, Eq. (5)	676 (3006)	676 (3006)	676 (3006)
	ACI 318-05, Eq. (4)	320 (1423)	320 (1423)	320 (1423)
	CCD method with $h_{ef}^{1.5}$ Eq. (1)	371 (1650)	371 (1650)	371 (1650)
	CCD method with $h_{ef}^{1.67}$ Eq. (3)	428 (1903)	428 (1903)	428 (1903)
Tests	Mean	733 (3260)	725 (3224)	509 (2264)
	COV, %	1.7	3.5	5.8
	5%-fractile	685 (3047)	625 (2780)	393 (1748)
	5%-fractile/ mean	0.93	0.86	0.77

Classification	Symbol in Fig. 9	Comparison	Ratio of observed to predictions (h_{ef} = 25 in. [635 mm])			
			T4	T5	T1	T4/T1
5% fractile of test results	(I)	$Nu_{,5\%}$/Eq. (5)	1.01	0.92	0.58	1.74
	(II)	$Nu_{,5\%}$/Eq. (5)	2.16	1.97	1.24	1.74
Mean of test results	(III)	Mean/Eq. (1)	1.98	1.96	1.37	1.45
	(IV)	Mean/Eq. (3)	1.71	1.70	1.19	1.44

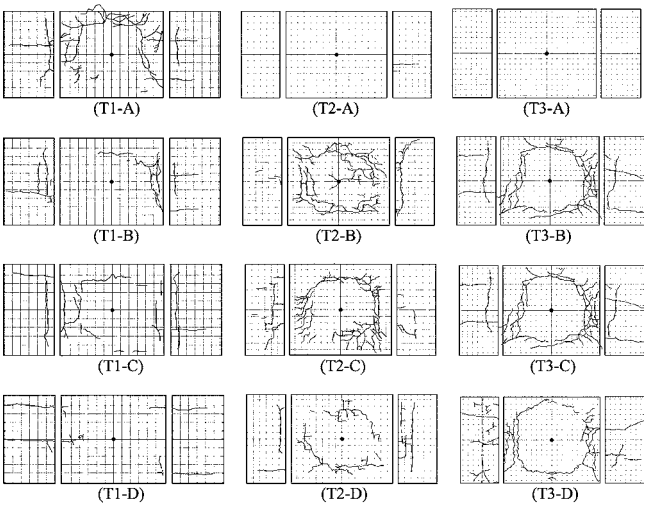

(a)

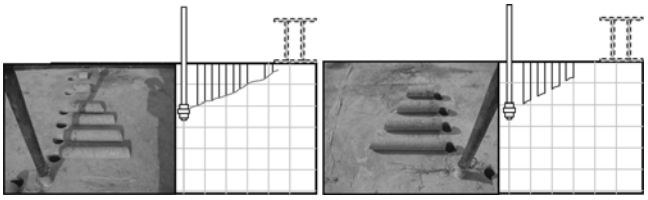

(b)

Fig. 6—(a) Cracking pattern for four test replicates (A, B, C, and D) of Specimens T1, T2, and T3; and (b) typical internal crack profile in Specimen T1.

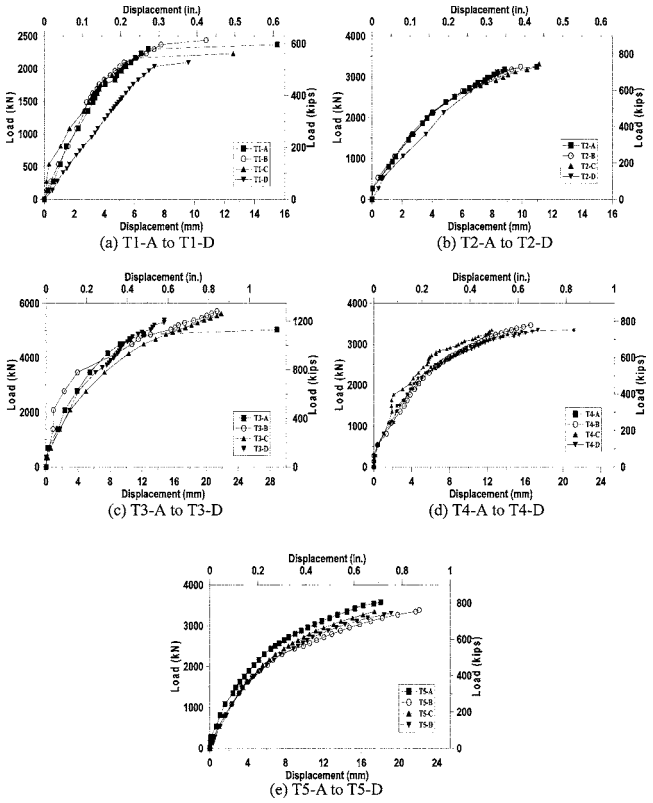

Fig. 7—Measured load-displacement relationships.

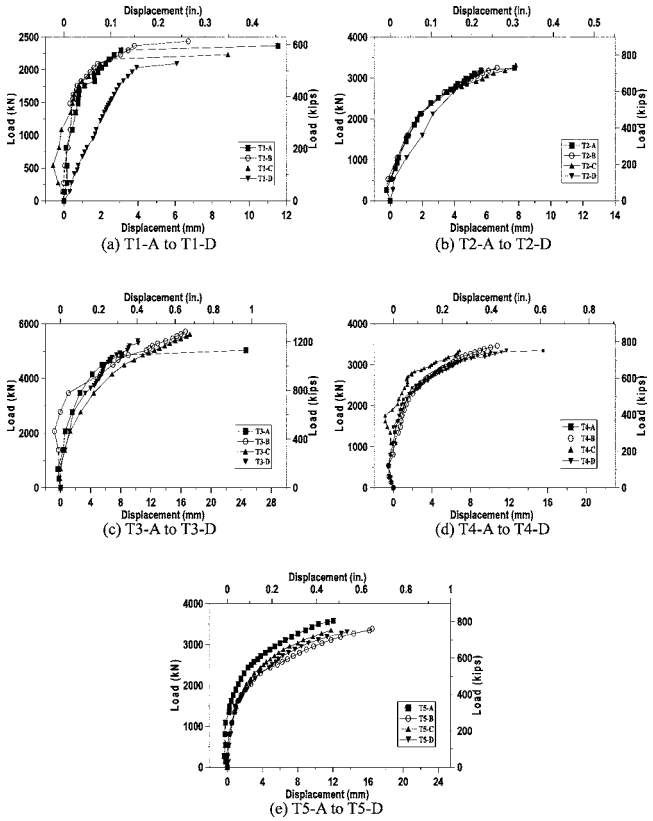

Fig. 8—Relation between load and anchor displacement at concrete surface.

caused by bending of the anchors if they were not installed perfectly perpendicular to the concrete surface. It can be seen that the anchor displacements at peak load of Specimens T1 to T3 (concrete cone failure) are rather small. This can be explained by the rather large anchor heads that, due to the low concrete stresses, did not slip much. For head sizes allowed by ACI 318-05, Appendix D, the breakout failure loads increase approximately proportional to $h_{ef}^{1.5}$. With much larger heads, the power on the embedment depths is greater than 1.5.[7] In the present tests, at failure, the related pressure under the head was on average p/f_c' = 4.37, 3.36, and 5.31 for test Series T1, T2, and T3. It was much smaller than the pressure allowed by ACI 318-05 for uncracked concrete ($p_n = 10f_c'$).

Comparison of predicted and tested tensile breakout capacities

In Table 3(a), tension test results for unreinforced Specimens T1, T2, and T3, and results in Table 3(b) for reinforced Specimens T4 and T5, are compared with predicted capacities. The measured mean failure loads are compared with the predicted mean capacities according to Eq. (1) and (3), respectively, and the 5%-fractiles of the measured failure loads calculated by assuming an unknown standard deviation are compared with the values according to Eq. (4) and (5). In Fig. 9, the ratios of measured capacities to predicted values are plotted. Figure 10 shows the measured failure loads of each test compared with the values predicted according to Eq. (5), Fig. 10(a); Eq. (1), Fig. 10(b); and Eq. (3), Fig. 10(c), as a function of the embedment depth. In Fig. 11, the measured concrete breakout loads, as well as the failure loads according to best fit equations using the current test results and Eq. (1), (2), (3), and (5), are plotted as a function of the embedment depth.

EVALUATION OF TEST RESULTS FOR UNREINFORCED SPECIMENS T1, T2, AND T3

According to the 45-degree cone model (Eq. (5)), the breakout capacities increase in proportion to h_{ef}^2. The predicted capacities $N_{u,calc}$ are much higher than the measure values $N_{u,test}$ and the ratio $N_{u,test}/N_{u,calc}$ decreases with increasing embedment depth (Fig. 10(a)). On average, the 5%-fractiles of the observed capacities are approximately half the capacities predicted by ACI 349-97 (Table 3(a)). This demonstrates that the 45-degree cone model is unconservative for deep anchors. This agrees with the findings by Fuchs et al.[3] and Shirvani et. al.[8] In contrast, the predictions according to the CCD method are conservative. The measured average breakout loads are approximately 30% higher than the values predicted according to Eq. (1) (N_u proportional to $h_{ef}^{1.5}$) with no significant influence of the embedment depth (Fig. 10(b)). On average, the ratio of measured failure loads to the values predicted by Eq. (3) (N_u proportional to $h_{ef}^{1.67}$) is 1.09 (Table 3(a)). It decreases slightly with increasing embedment depth (Fig. 10(c)).

In Fig. 10(d) to 10(f), the breakout failure loads of headed anchors with an embedment depth $h_{ef} \geq 8$ in. (200 mm) measured in the present tests and taken from other sources[3,8] are compared with values predicted by the CCD method. According to Fig. 10(d), the prediction according to Eq. (1) is conservative for large embedment depths. The failure loads predicted by Eq. (3) agree quite well with the measured values (Fig. 10(e)). Figure 10(f) shows that the CCD method changing the exponent on h_{ef} from 1.5 to 1.67 at an effective embedment depth of 10 in. (250 mm) predicts the failure loads of anchors with $h_{ef} \geq 8$ in. (200 mm) best. Only two

test points at h_{ef} = 8 in. (200 mm) fall below the assumed 5%-fractile, which is equal to 75% of the average value.

The 5%-fractiles of the capacities observed in the present tests average approximately 120% of the values predicted by ACI 318-05, Appendix D (Eq. (4)) (refer to Table 3(a)). The higher ratio $N_{u,test}/N_{u,calc}$ when comparing the 5% fractiles with each other instead of the average values is due to the rather low scatter of test results. On average, the coefficient of variation (COV) was approximately 5%. This results in an average ratio $N_{u,5\%}/N_{u,m}$ of 0.81, whereas in ACI 349-01, a ratio of 0.75 is assumed. In actual structures, the concrete strength, and thus the concrete cone resistance, might vary more than in the present test specimens. Therefore, the ratio $N_{u,5\%}/N_{u,m}$ assumed in ACI 318-05, Appendix D, should be maintained.

Numerical investigations by Ozbolt et al.[7] using a sophisticated three-dimensional nonlinear finite element model demonstrates that the concrete breakout capacity of headed anchors is influenced by the head size, that is, the pressure under the head, related to the concrete compressive strength as described previously.

Based on the previous evaluations, it is recommended to predict the nominal concrete breakout capacities of anchors with an embedment depth $h_{ef} \geq 10$ in. (250 mm) in uncracked concrete by Eq. (4). Equation (4) is valid, however, only if the head size is large so that the pressure under the head at the nominal capacity is $p_n \leq 3f_c'$. This limiting value is deduced from the results of the test Series T1 to T3. In these tests, the pressure under the head was p_n/f_c' = 3.4 to 5.3, on average 4.3. The nominal capacity is approximately 75% of the mean capacity (compare Eq. (4) with Eq. (3)). When applying this reduction factor, one gets p_n/f_c' = 3.2 ~ 3.0. This limiting value is supported also by the numerical analysis results.[7] For smaller heads, for which the nominal pressure under the head is $p_n > 3f_c'$, the breakout capacities in uncracked concrete should be predicted by Eq. (2).

In cracked reinforced concrete, lower breakout capacities than in uncracked concrete are observed.[9] Therefore, ACI 318-05, Appendix D, reduces the nominal breakout capacities of headed anchors in cracked reinforced concrete by a factor 0.8 compared with uncracked concrete. Therefore, in cracked concrete Eq. (4) with $h_{ef}^{1.67}$, multiplied by the factor 0.8, should only be used for deep anchors if the pressure under the head is $p_n \leq 2.4f_c'$.

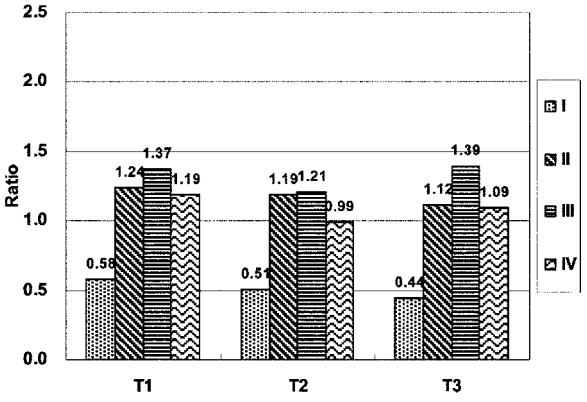

(a) Unreinforced specimens (T1, T2, and T3).

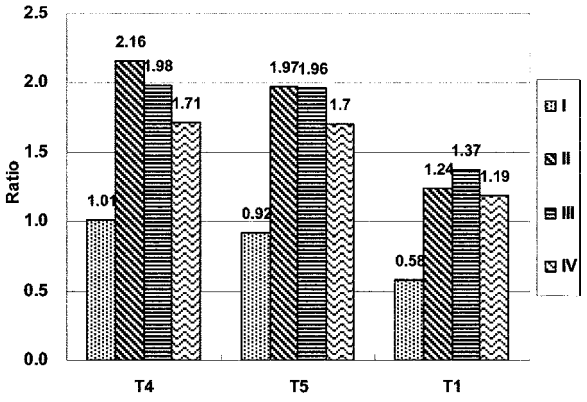

(b) Reinforced specimens (T4 and T5)

Fig. 9—Ratios of test results (5% fractile and mean) to predicted capacities; compare with Table 3.

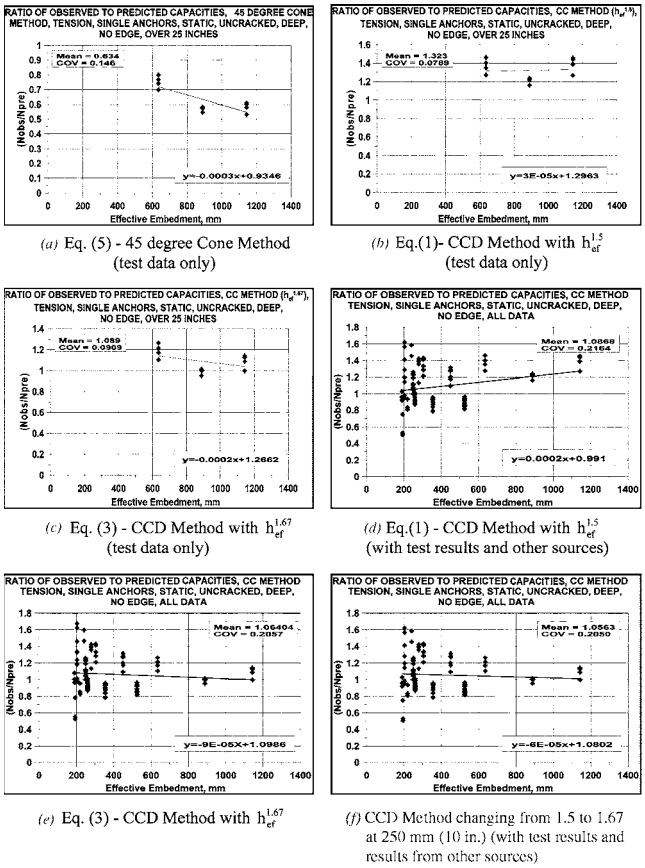

(a) Eq. (5) - 45 degree Cone Method (test data only)

(b) Eq.(1)- CCD Method with $h_{ef}^{1.5}$ (test data only)

(c) Eq. (3) - CCD Method with $h_{ef}^{1.67}$ (test data only)

(d) Eq.(1) - CCD Method with $h_{ef}^{1.5}$ (with test results and other sources)

(e) Eq. (3) - CCD Method with $h_{ef}^{1.67}$

(f) CCD Method changing from 1.5 to 1.67 at 250 mm (10 in.) (with test results and results from other sources)

Fig. 10—Ratios of observed to predicted concrete tensile breakout capacities as function of embedment depth.

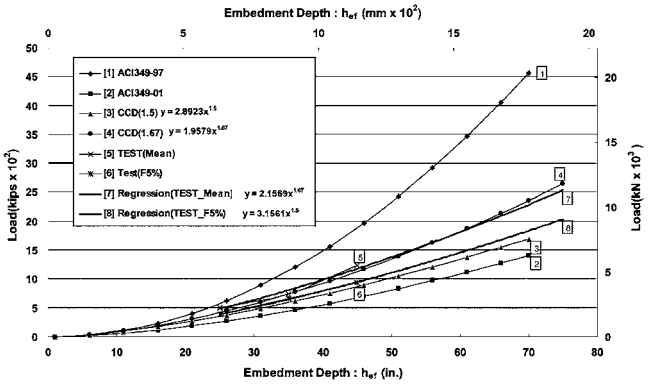

Fig. 11—Test results and comparison with predicted capacities.

EFFECT OF SUPPLEMENTARY REINFORCEMENT

Reinforced Specimen T4

Test Specimens T4, with supplementary reinforcement, are shown in Fig. 3. The mean tested failure load (733 kips [3260 kN]) is close to the sum (806 kips [3585 kN]) of the calculated reinforcement strength (378 kips [1681 kN]) and the unreinforced concrete strength (428 kips [1904 kN]) by Eq. (3). It can be inferred that the adopted reinforcement pattern effectively acted in the anchorage system to resist tension load.

The tested breakout strength of the unreinforced test Specimen T1 with the same embedment depth as Specimen T4 was 509 kips (2264 kN). Comparison of the mean tested strengths of Specimens T1 and T4 shows that the effective increase in capacity due to supplementary reinforcement is roughly 224 kips (996 kN), or approximately 60% of the calculated yield strength of the supplementary reinforcement.

The loading on Specimen T4-A was increased to the expected total yield force of the supplementary reinforcement so that the load distribution to each of the two reinforcement groups could be estimated. The load resisted by the supplementary reinforcement in the inner concentric circle (4.2 in. [106 mm] from the axis of the anchor) was 2.2 times the load resisted by the equal area of supplementary reinforcement in the outer concentric circle (8.5 in. [216 mm] from the axis of the anchor).

According to the measured strains in the strain gauges attached to reinforcing bars, the reinforcing bars close to the anchor were more effective in increasing the tensile capacity and their maximum stress was measured close to the anchor head.

Reinforced Specimen T5

The mean tested capacity (725 kips [3225 kN]) of the four replicates of test Specimen T5, with supplementary reinforcement as shown in Fig. 3 was much smaller than the sum (1129 kips [5021 kN]) of the calculated reinforcement strength, 16 x 60 ksi x 0.79 in.^{2} = 758 kips (3371 kN) and concrete breakout strength per the CCD method given by Eq. (1), 371 kips (1650 kN). These test results indicate that this layout of supplementary reinforcement contributes with a low level of effectiveness to the capacity of the anchor. This conclusion is corroborated by measured strains in the gauges attached to the reinforcing bars, which indicates little strain in the reinforcement. As noted previously, however, Specimen T5 were not fully loaded up to failure due to safety concerns. As a consequence, the results of Series T5 are judged to not be useful in verifying the absolute effectiveness of the supplementary reinforcement. By comparing results from Specimens T4 with those of Specimens T5, however, it is still possible to judge the relative effectiveness of the different supplementary reinforcement patterns. For a given applied load, stresses in the supplementary reinforcement of Specimens T5 along the outer circles are less than half of those along the inner circle. The relative trends of stress distribution are similar for each reinforcement in both Series T4 and T5. Therefore, it can be inferred that the increase in tensile capacity is approximately proportional to the amount of supplementary reinforcement.

The load-displacement curves of Series T4 show that the peak load was nearly reached in the tests. In Series T5, the load could still be increased. In Series T4, the supplementary reinforcement was not strong enough to resist the concrete breakout load. In Series T5, the loading was stopped before the supplementary reinforcement could be fully activated. Therefore, it is not possible to formulate a general model from the test results. The results, however, show that with supplementary reinforcement arranged as in Specimens T4 and dimensioned for about 80 to 100% of the expected ultimate concrete breakout capacity, the failure load was increased by approximately 50% over the unreinforced case. This result can reasonably be used in the calculation of ultimate strength.

SUMMARY AND CONCLUSIONS

Tensile load-displacement behavior of large anchors without supplementary reinforcement

The test results show that ACI 349-97 (Eq. (5)) significantly overestimates the tensile breakout capacity of large anchors. The ratio $N_{u,test}/N_{u,calc}$ decreases with increasing embedment depth (Fig. 10(a)). Furthermore, the slope of the concrete cone was much flatter than 45 degrees. Therefore, the overestimation of the failure loads would be even larger for anchors at an edge or for anchor groups. For these reasons, this formula in ACI 349-97 should not be used in design.

The CCD method with $h_{ef}^{1.5}$ (Eq. (1)) is conservative for large anchors (Fig. 10(b)). This is probably due to the fact that this method is based on linear fracture mechanics, which is valid only for anchors with high bearing pressure, that is, anchors with small heads. The tested anchors, however, had rather large heads. The test results can best be predicted by the CCD method with (Eq. (3)) (refer to Fig. 9 and 10(e)). On average, the measured failure loads are approximately 10% higher than the predicted values. If all available results are taken into account (refer to Fig. 10(f)), however, a change of Eq. (3) seems not to be justified.

It is proposed to calculate the characteristic resistance of single anchor bolts with $h_{ef} \geq 10$ in. (250 mm) and low bearing pressure (pressure under the head at nominal breakout load $p_n \leq 3f_c'$ [uncracked concrete] or $p_n \leq 2.4f_c'$ [cracked concrete]) according to ACI 318-05, Appendix D, or ACI 349-01, Appendix B, using the equation with $h_{ef}^{1.67}$). According to the test results, however, the average cone angle was not 35 degrees (as assumed in the CCD method) but only approximately 25 to 30 degrees. Therefore, the characteristic spacing $s_{cr,N}$ and characteristic edge distance $c_{cr,N}$ are probably larger than $s_{cr,N} = 2c_{cr,N} = 3h_{ef}$ as assumed in ACI 318-05. Therefore, it seems prudent to calculate the resistance of anchorages at an edge or corner, or of group anchorages, according to ACI 318-05, but with $s_{cr,N} = 4.0\ h_{ef}$ instead of $s_{cr,N} = 3.0\ h_{ef}$ as given in ACI 318-05.

Tensile load-displacement behavior of large anchors with supplementary reinforcement

In Series T4, the supplementary reinforcement was not strong enough to resist the applied load. Even in Test T4-A, in which the supplementary reinforcement yielded, only approximately 1/3 (246/759 ≈ 0.33) of the applied peak load was resisted by the reinforcement. In Series T5, which had a stronger reinforcement, the tests had to be stopped because of tensile yielding of the anchors before the supplementary reinforcement had been fully mobilized. Therefore, the results of these tests cannot be used to develop a general design model for anchors with supplementary reinforcement.

Nevertheless, the results of test Series T4 showed that the peak load could be increased by approximately 50% compared with the results from test Series T1 without supplementary reinforcement. Therefore, it is proposed to increase the concrete breakout resistance calculated as described

previously by a factor of 1.5 if supplementary reinforcement is present around each anchor of an anchor group. The supplementary reinforcement must be arranged as in Tests T4 (four U-shaped stirrups at a distance ≤ 4 in. (100 mm) or ≤ $0.15h_{ef}$ from the anchor) and dimensioned for the characteristic concrete breakout resistance according to Eq. (4)).

In a more general model, the supplementary reinforcement should be dimensioned to take up 100% of the applied load, thus neglecting the contribution of the concrete. The supplementary reinforcement should be designed using a strut-and-tie model. The characteristic resistance of the supplementary reinforcement is given by the bond capacity of the supplementary reinforcement in the anticipated concrete cone, which should be assumed to radiate from the head of the anchor at an angle of 35 degrees. The bond capacity should be calculated according to codes of practice (for example, ACI 318-05[1] or Eurocode 2[10]). The design strength is limited by the yield capacity of the bars. This model is described in detail in References 11 and 12.

ACKNOWLEDGMENTS

The authors would like to acknowledge the financial and technical help of Korea Hydro & Nuclear Power Co. Ltd. and Korea Electric Power Research Institute for financing this research work and several on-going research projects related to the capacity of anchorage to concrete structures. The authors are also grateful for the valuable advice of R. Eligehausen, University of Stuttgart, Stuttgart, Germany; R. Klingner, University of Texas at Austin, Austin, Tex.; and members of ACI Committee 355, Anchorage to Concrete.

REFERENCES

1. ACI Committee 318, "Building Code Requirements for Structural Concrete (ACI 318-05) and Commentary (318R-05)," American Concrete Institute, Farmington Hills, Mich., 2005, 430 pp.

2. ACI Committee 349, "Code Requirements for Nuclear Safety-Related Concrete Structures (ACI 349-01)," American Concrete Institute, Farmington Hills, Mich., 2001, 134 pp.

3. Fuchs, W.; Eligehausen, R.; and Breen, J. E., "Concrete Capacity Design (CCD) Approach for Fastening to Concrete," *ACI Structural Journal*, V. 92, No. 1., Jan.-Feb. 1995, pp. 73-94.

4. Rehm, G.; Eligehausen, R.; and Mallée, R., "Befestigungstechnik" (Fastening Technique), *Betonkalender 1995*, Ernst & Sohn, Berlin, Germany, 1995.

5. Comité Euro-International du Beton, "Fastening to Reinforced Concrete and Masonry Structures," *State-of-the-Art Report*, CEB, Thomas Telford, London, 1991, pp. 205-210.

6. ACI Committee 349, "Code Requirements for Nuclear Safety Related Concrete Structures (ACI 349-97)," American Concrete Institute, Farmington Hills, Mich., 1997, 123 pp.

7. Ozbolt, J.; Eligehausen, R.; Periskic, G.; and Mayer, U., "3D FE Analysis of Anchor Bolts with Large Embedment Depths," *Fracture Mechanics of Concrete Structures*, V. 2, No. 5, Apr. 2004, Vail, Colo., pp. 845-852.

8. Shirvani, M.; Klingner, R. E.; and Graves III, H. L., "Behavior of Tensile Anchors in Concrete: Statistical Analysis and Design Recommendations," *ACI Structural Journal*, V. 101, No. 6, Nov.-Dec. 2004, pp. 812-820.

9. Eligehausen, R., and Balogh, T., "Behavior of Fasteners Loaded in Tension in Cracked Reinforced Concrete," *ACI Structural Journal*, V. 92, No. 3, May-June 1995, pp. 365-379.

10. Eurocode 2, "Design of Concrete Structures, Part 1: General Rules and Rules for Buildings," 2004.

11. Technical Committee CEN/TC 250, "Design of Fastening for Use in Concrete, Part 2: Headed Fasteners," Final Draft, CEN Technical Specifications, 2004.

12. Comité Euro-International du Beton (CEB), *Design Guide for Anchorages to Concrete*, Thomas Telford, London, 1997.